SUPPLEMENTARY FIGURE LEGENDS

Supplementary Figure S1 Deletion of the SNAG domain abolishes the transcriptional repressive function of Snail1. (A) Vector, WT- or ΔSNAG-Snail1 were co-expressed with the E-cadherin promoter luciferase construct in MCF7 cells. After 42 hr, cells were treated with MG132 for 6 hours and luciferase activity was measured using the Dual-Luciferase Reporter Assay (Promega) (mean ± SD of three separate experiments) (bottom panel). (B) Input lysates from above were analyzed for the expression of Snail1 and actin by Western blotting.

Supplementary Figure S2 The SNAG domain of Snail1 does not alter the subcellular localization of Snail1. (**A**) d2-GFP or SNAG-d2-GFP was expressed in HEK293 cells. The subcellular localization of d2-GFP (green) was visualized by immunofluorescence microscopy (Dapi for nuclei, red) and assessed in 200 cells at 4 different views. The bar graph shows the percentages of cells with the indicated subcellular localization. (**B**) EGFP-tagged WT or SNAG-deleted Snail1 was expressed in HEK293 cells. The subcellular localization of Snail1 (green) was visualized by immunofluorescence microscopy (Dapi for nuclei, red) and assessed as described above.

Supplementary Figure S3 The SNAG domain of Snail1 does not affect the subcellular localization of Snail1. d2-GFP or SNAG-d2-GFP and WT or SNAG-deleted Snail1 was expressed in HeLa cells. The subcellular localization of d2-GFP (top panel) and Snail1 (bottom panel) were analyzed by cellular fractionation. Tubulin and poly-adenosine ribose polymerase (PARP) were used as markers of the cytoplasmic and nuclear fractions, respectively.

Supplementary Figure S4 Proline 2, arginine 3, lysine 9, and proline 10 in the SNAG domain of Snail1 are critical for the stability of Snail1. WT and mutant Snail1s were expressed in HEK293 cells treated with or without MG132 (10 μM) for 6 h. The level of Snail1 was examined by Western blotting.

Supplementary Figure S5 The transcriptional repressive function of Snail1 is correlated with its interaction with LSD1. Vector, WT or SNAG-domain mutants of Snail1 were co-expressed with the E-cadherin promoter luciferase construct in MCF7 cells. After 48 hr, luciferase activity was measured using a Dual-Luciferase Reporter Assay (Promega) (mean ± SD of three separate experiments) (bottom panel).

Supplementary Figure S6 Detection of Snail1 methylation. Snail1 was expressed in HEK293 cells and treated with or without TSA (10 μM) for 12 h. After Snail1 was immunoprecipitated, separated on SDS-PAGE, and transferred to a membrane, the methylation of Snail1 was examined using antibodies against the methylation of H3K4 and H3K9.

Supplementary Figure S7 Input lysates from Figures 4B and 4C were analyzed for the expression of different deletion mutants of LSD1 and Snail1 by Western blotting.

Supplementary Figure S8 Mutation of the critical residues that interact with histone H3 in the catalytic pocket of LSD1 disrupt the interaction of LSD1 with Snail1 (**A**) The schematic diagram shows the positions of D375, E379, D553, D555 and D556 that interact with the arginine 8 (R8) and arginine 2 (R2) of histone H3, respectively. (**B**) Flag-tagged wild-type or mutant LSD1 were co-expressed with HA-tagged Snail1 in HEK293 cells. After immunoprecipitation of LSD1 and Snail1, the bound Snail1 and LSD1 were analyzed by Western blotting, respectively.

Supplementary Figure S9 Input lysates from Figure 5B were analyzed for the expression of LSD1, CoREST and Snail1 by Western blotting.

Supplementary Figure S10 Input lysates from Figure 7A (A) and Figure 7B (B) were analyzed for the expression of LSD1 and Snail1 by Western blotting.

Supplementary Figure S11 Input lysates from HCT116, PC3 and MDA-MB231 cells in Figure 7C were analyzed for the expression of LSD1, CoREST and Snail1 by Western blotting.

Supplementary Figure S12 LSD1 is critical for the repressive function of Snail1. Snail1, LSD1 and non-target control siRNA were expressed in HCT116, PC3, and MDA-MB231 cells as described above. After 48 h, a scratch ("wound") was induced in a cell monolayer and cell culture was continued. Images were obtained at the beginning and at the 48 hr time point to compare the cell migration for the closure of the wound. The statistical analysis for the migration of HCT116 and MDA-MB231 is shown in the bar graph (**A**). The statistical analysis for the migration of PC3 cells was presented in Figure 7D. (**B**) Representative images from PC3 cells are shown (experiments were performed at least twice). Scale bar = 200 μm.

Supplementary Figure S13 The invasive ability of PC3 and MDA-MB231 cells with knockdown of either Snail1, LSD1, CoREST, or both of Snail1 and LSD1 was analyzed by the invasion assay. Invaded cells from 6 different view areas were counted and plotted as bar graph (mean ± SEM of two separate experiments).

Supplementary Figure S1

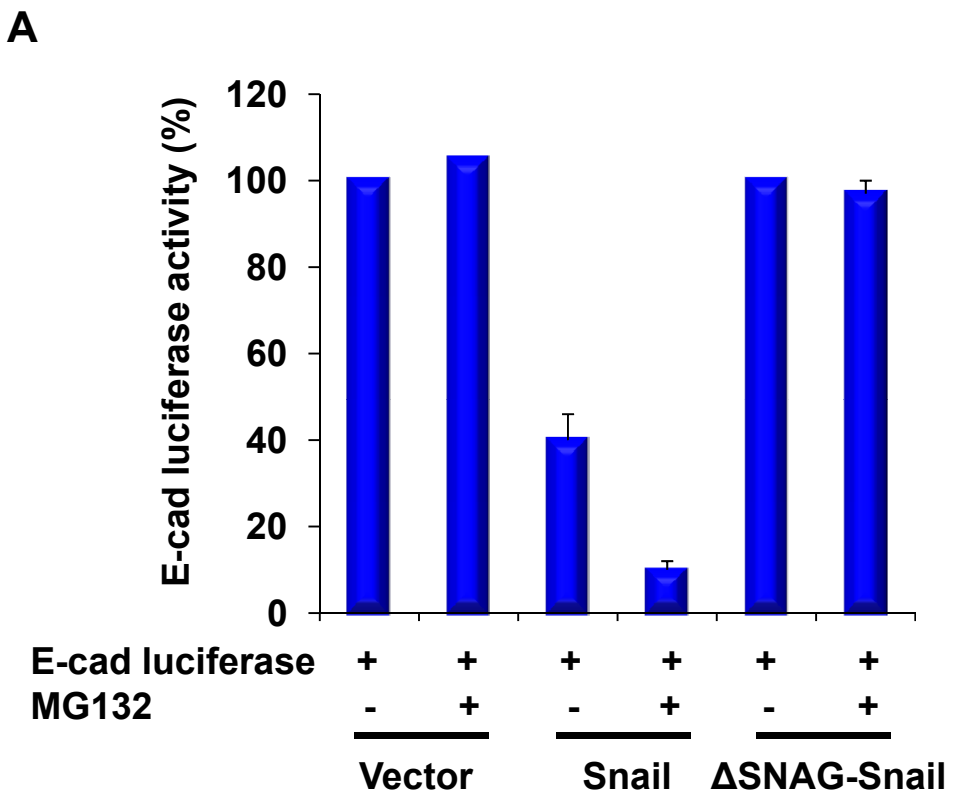

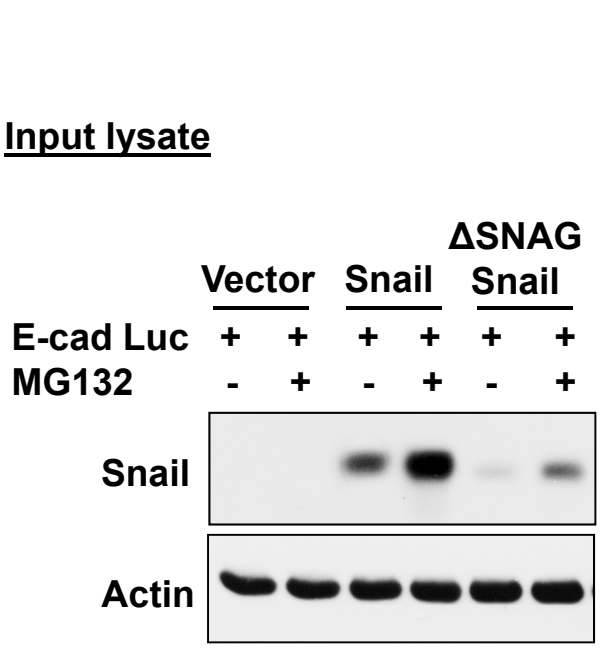

Supplementary Figure S2

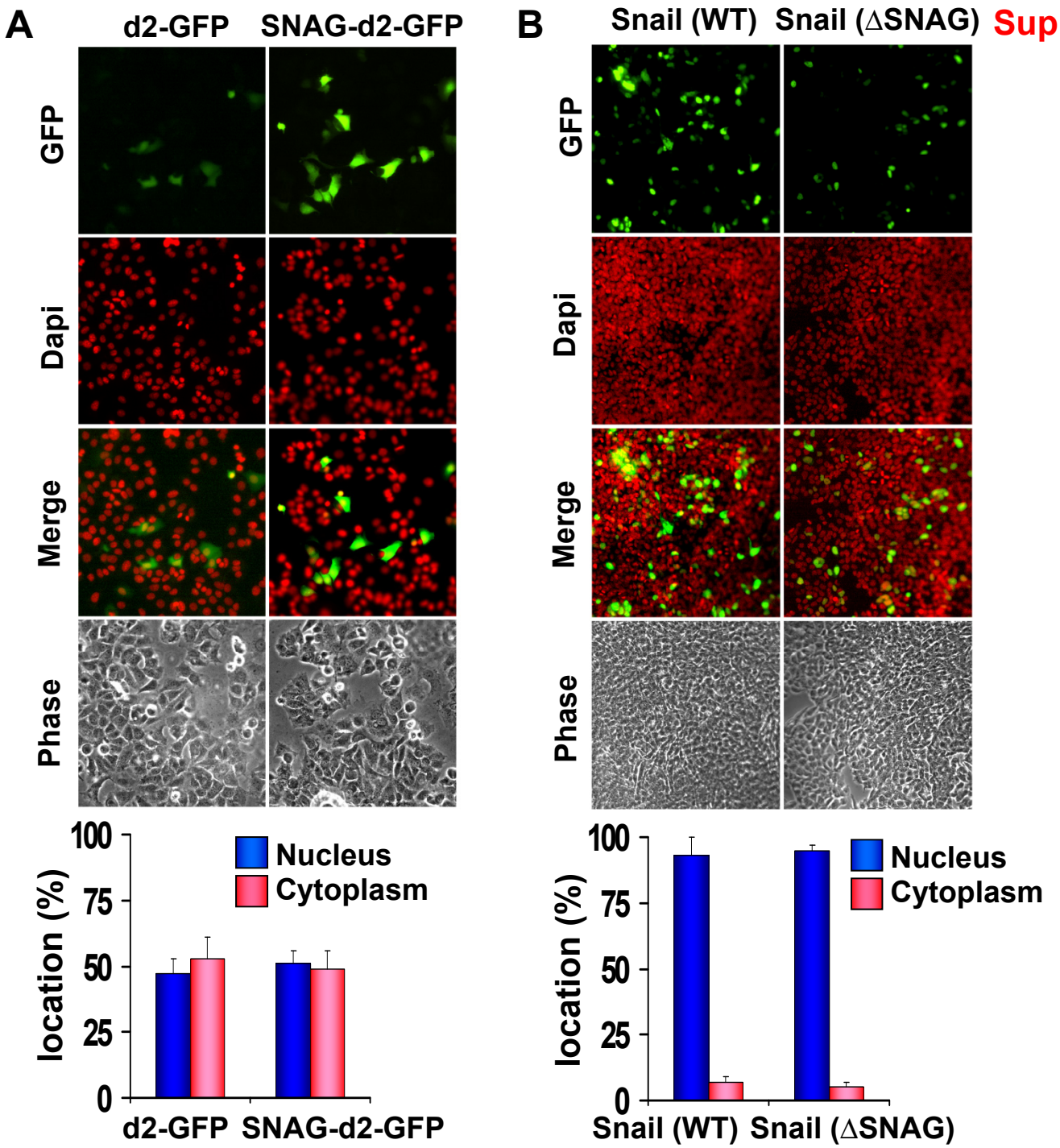

Supplementary Figure S3

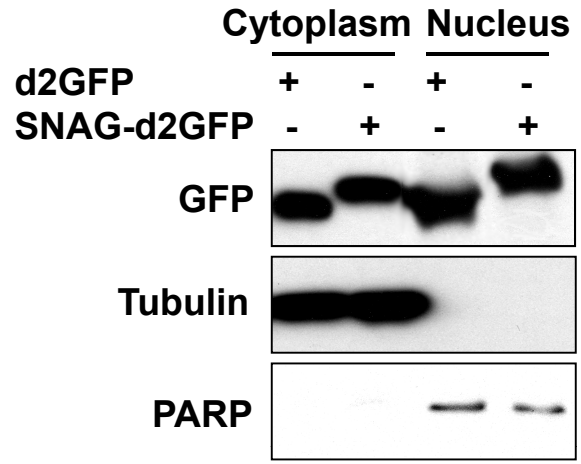

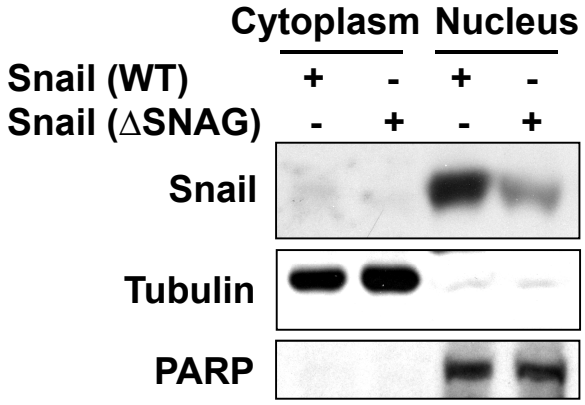

Supplementary Figure S4

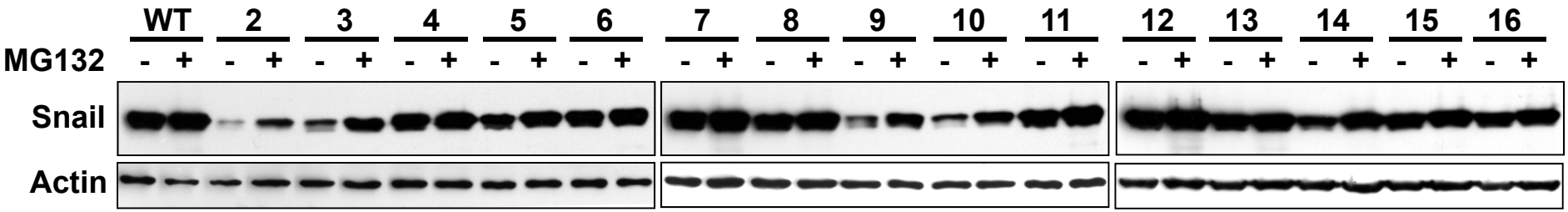

Supplementary Figure S5

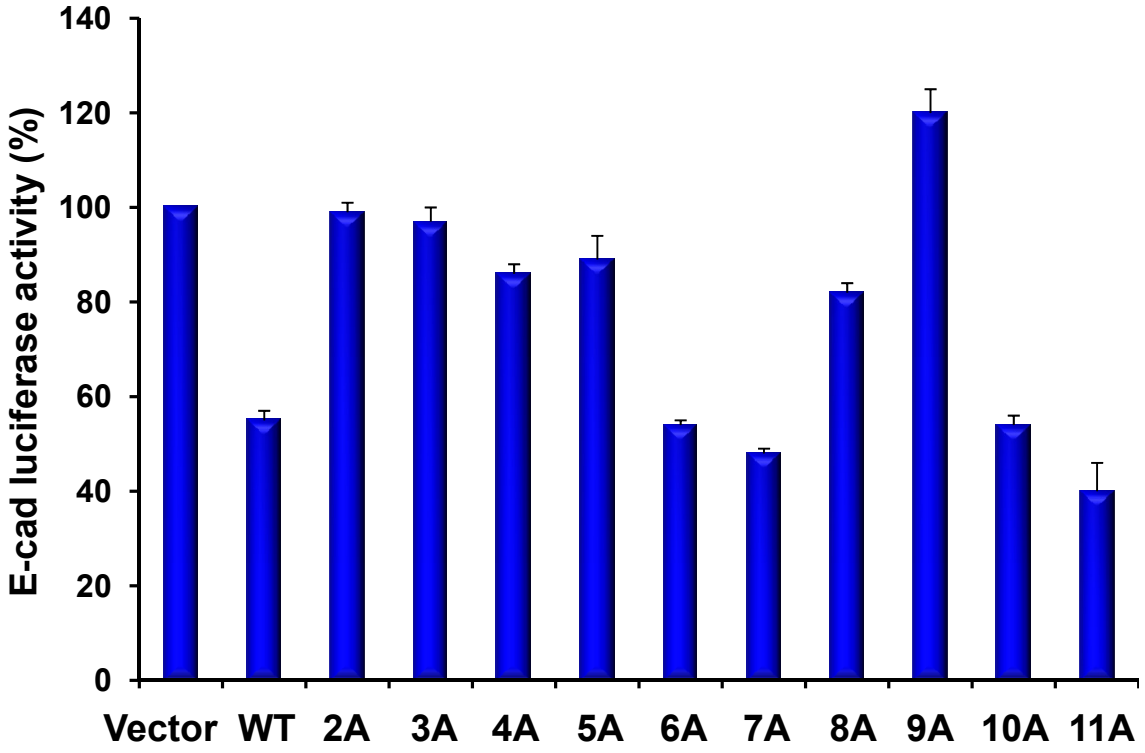

Supplementary Figure S6

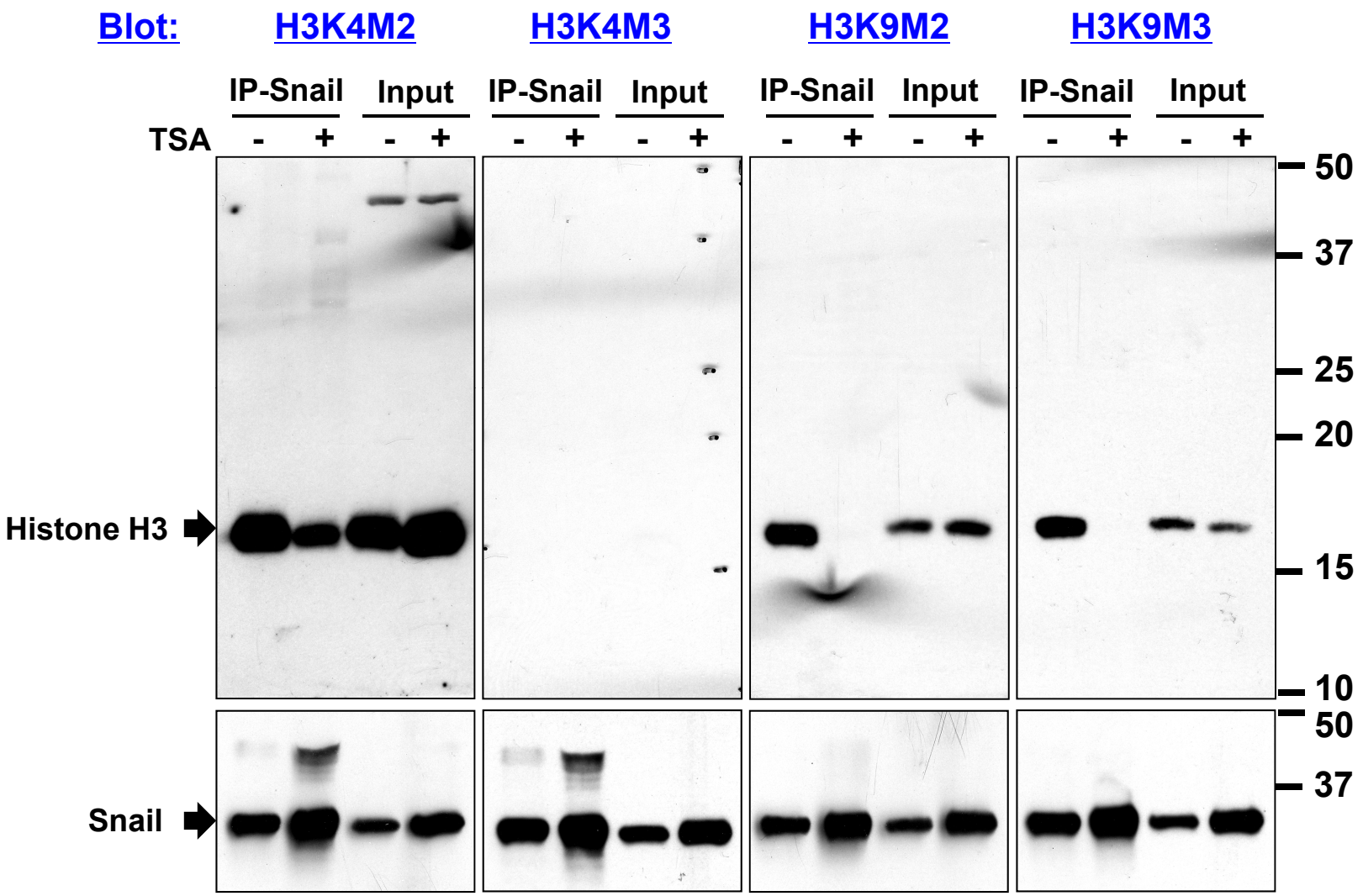

Supplementary Figure S7

Input for Figures 4B & 4C

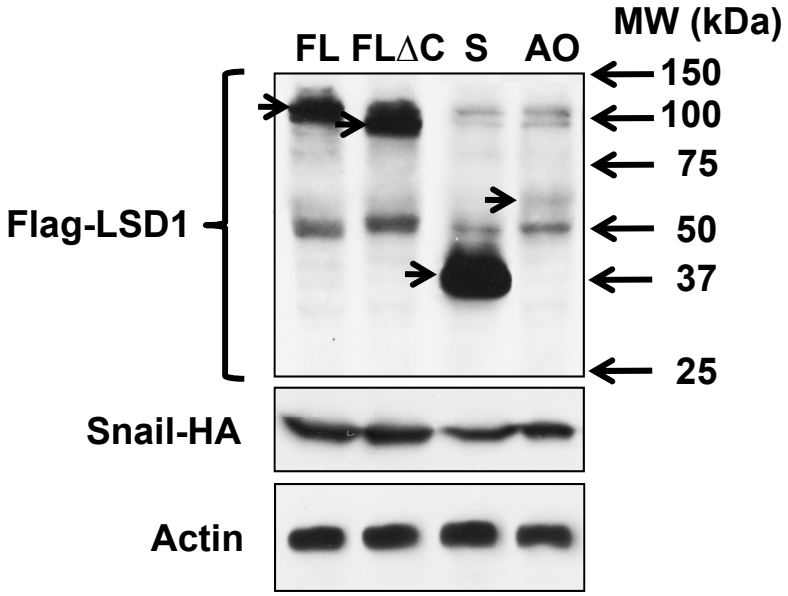

Supplementary Figure S8

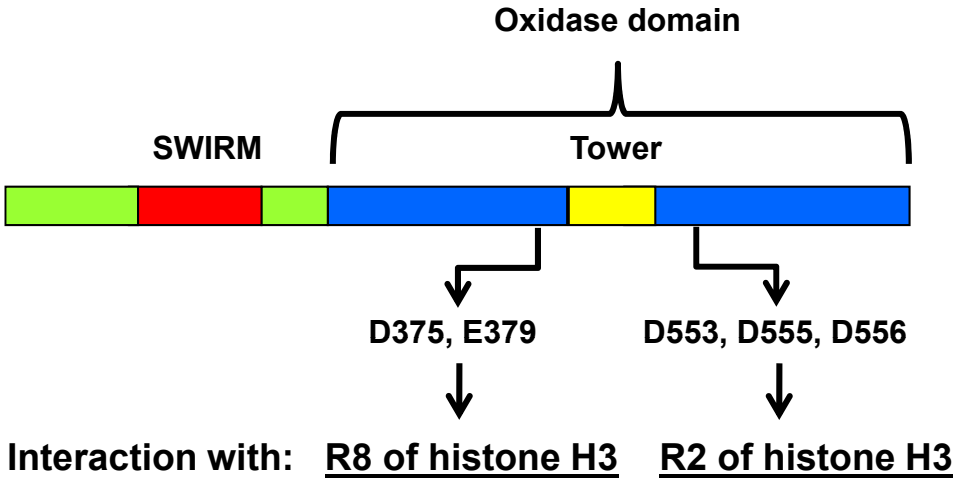

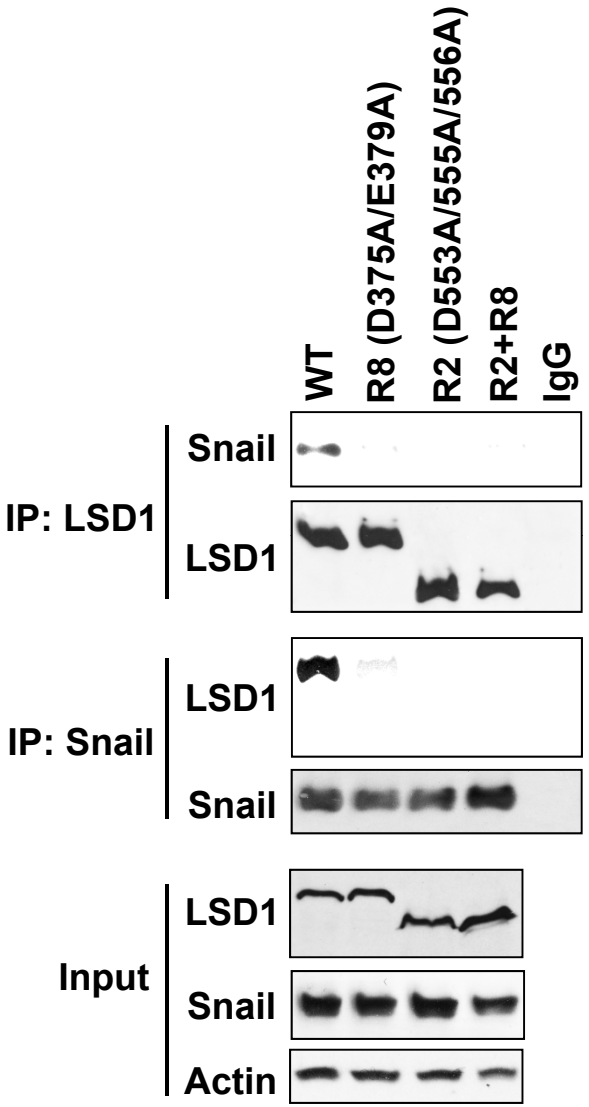

Supplementary Figure S9

Input for Figure 5B

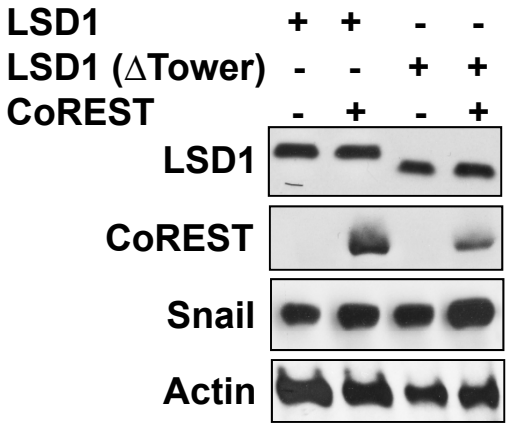

Supplementary Figure S10

A

Input for Figure 7A

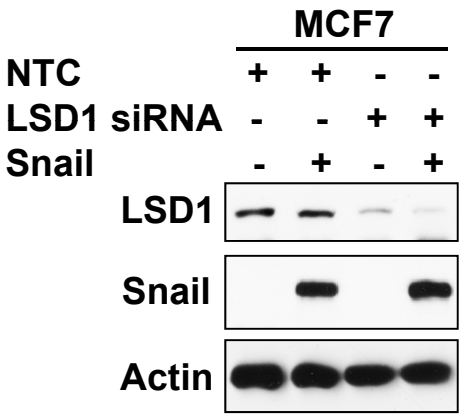

B

Input for Figure 7B

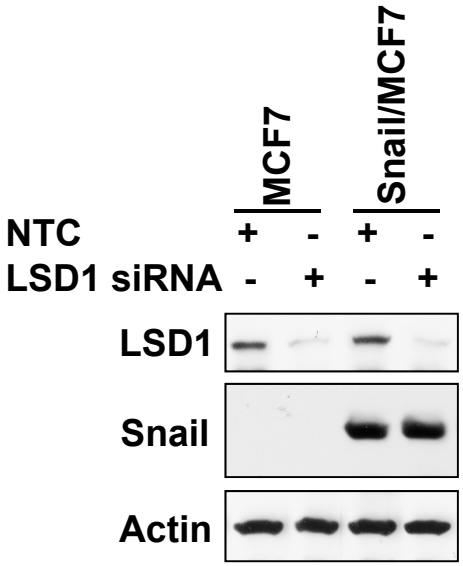

Supplementary Figure S11

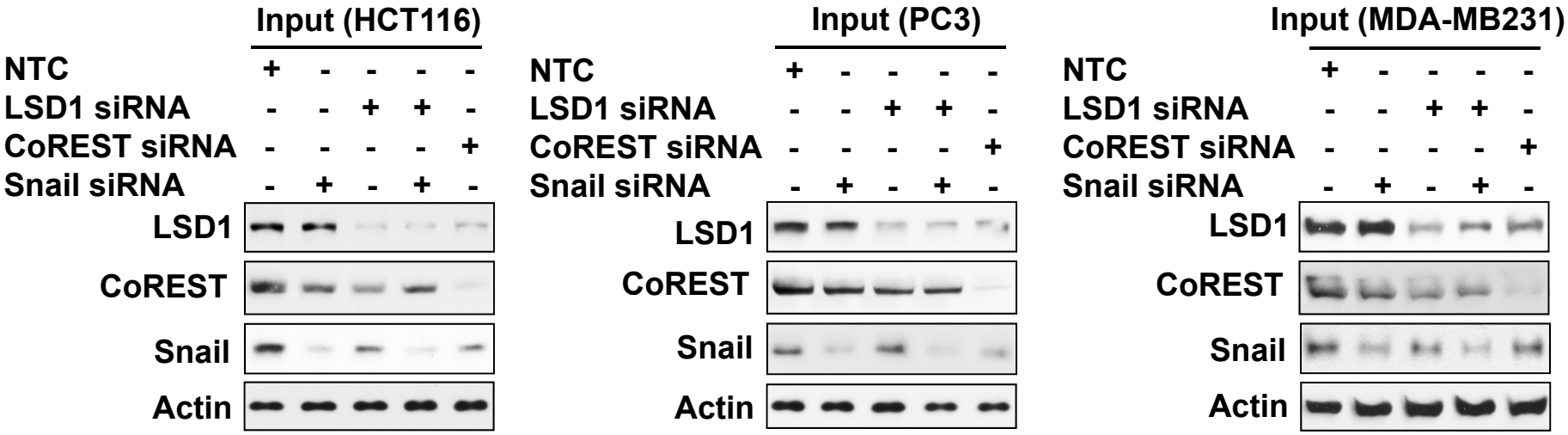

Supplementary Figure S12

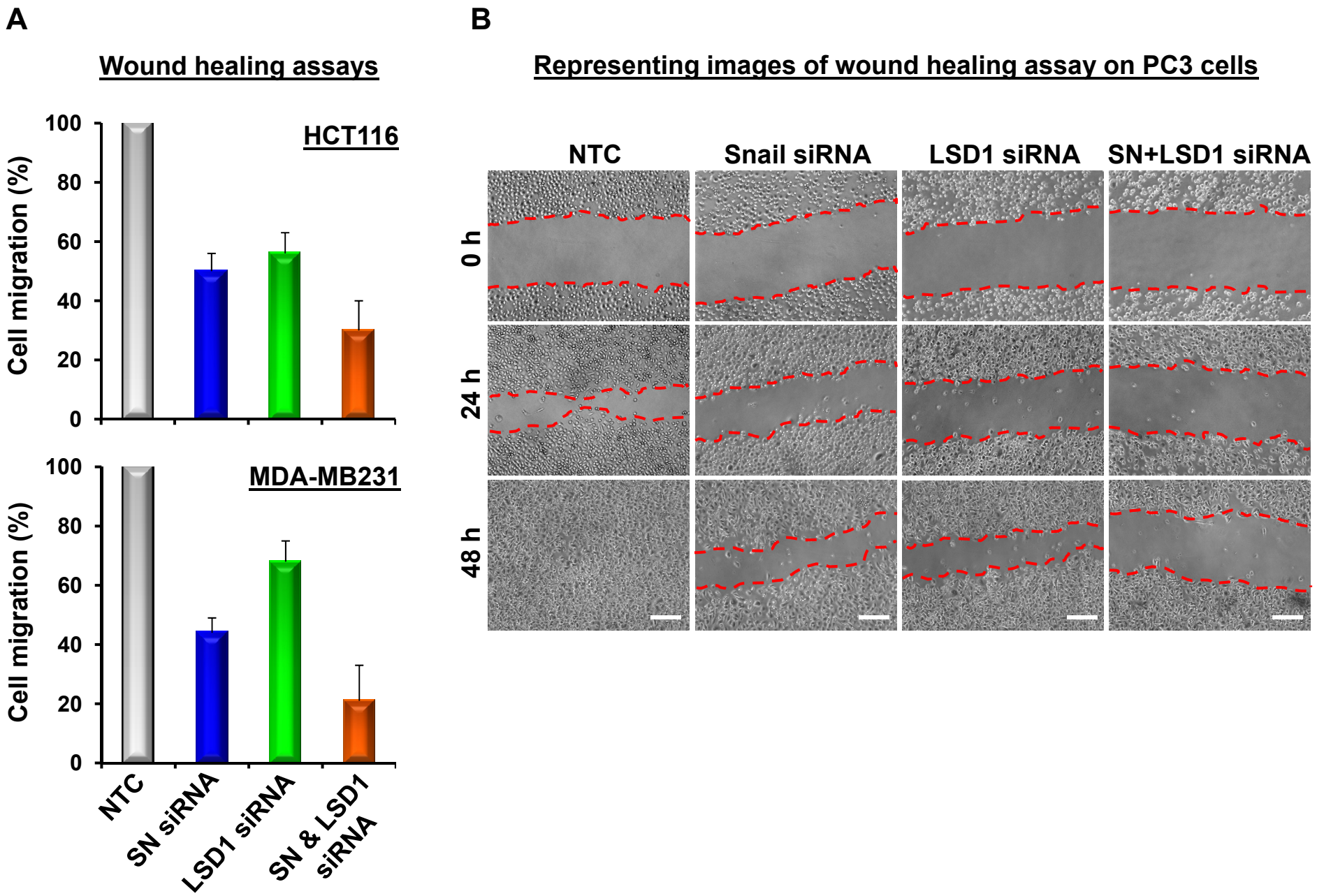

Supplementary Figure S13